Supporting Information to

Ru@MnO_2 core@shell nanowires as bifunctional electrocatalyst for efficient solar-driven seawater splitting

Na Li,[a] Aitong Yang,[a] Mengyuan Jin,[a] Shun Wang,[a] Ping Yu,[b,*] Juan Wang,[a,*] and Huile Jin,[a,*]

[a]Wenzhou Key Lab of Advanced Energy Storage and Conversion, Zhejiang Province Key Lab of Leather Engineering, College of Chemistry and Materials Engineering, Wenzhou University, Wenzhou, Zhejiang 325035, China.

[b]Technological Institute of Materials & Energy Science (TIMES), Xi'an Key Laboratory of Advanced Photo-electronics Materials and Energy Conversion Device, Xijing University, Xi'an, 710123, China.

* Corresponding author: Juan Wang: juanwang@wzu.edu.cn;

Ping Yu: yupingtina1128@126.com

Huile Jin: huilejin@wzu.edu.cn

Experimental Procedures

1. Materials

Sodium chloride (NaCl, AR, 99.5%) and Isopropyl alcohol (C_3H_8O, ≥99.5%) were obtained from Shanghai Meryer. Ruthenium (III) chloride hydrate ($RuCl_3·H_2O$, 97%, Ru: 37%, RG) was purchased from Adamas. Manganese Dioxide ($MnSO_4·H_2O$, AR) was bought from Shanghai Dibo Biotechnology Co., LTD. Potassium persulfate ($K_2S_2O_8$, 99.9%) was purchased from Macklin. Potassium permanganate ($KMnO_4$, AR) was acquired from Zhejiang Zhongxing Chemical Reagent Co., LTD.

2. Preparation of α-MnO_2 NWs

Typically, 0.13 g of $MnSO_4·H_2O$ and 0.33 g of $KMnO_4$ were dissolved in 20 mL of ultrapure water under magnetic stirring. The mixture was then transferred to a 40 mL Teflon-lined autoclave for heat treatment at 160 °C for 12 h. After cooling to room temperature, the precipitate was centrifuged and washed three times with ultrapure water and alcohol. After drying overnight in an oven at 80 °C, the final product of α-MnO_2 was collected.

3. Preparation of β-MnO_2 NWs

Typically, 0.73 g of $MnSO_4·H_2O$ and 1.16 g of $K_2S_2O_8$ were dissolved in 20 mL of water and then homogenized by ultrasound. The mixture was then transferred to a 40 mL Teflon-lined autoclave and heated in an oven at 160 °C for 24 h. After cooling, the sediment was centrifuged and washed three times with ultrapure water and alcohol. After drying overnight, the final product of β-MnO_2 was obtained.

4. Preparation of Ru@MnO_2 NWs

Typically, 12.50 mg of MnO_2 NWs and 10 mg of $RuCl_3·xH_2O$ are separately dispersed in 2.5 mL of water. After ultrasonic treatment for half an hour to create a uniform dispersion, the $RuCl_3$ solution was added to the MnO_2 NWs solution and further subjected to ultrasonic treatment. The obtained product is then dried in an oven at 80°C. Subsequently, the dried product was annealed in an Ar atmosphere at 300 °C for 2 h to obtain Ru@MnO_2 NWs.

3. Characterization

X-ray diffraction (XRD) patterns was performed on Bruker D8 ADVANCE X-ray diffractometer equipped with Cu Kα radiation source (λ=1.5418 Å). X-ray photoelectron spectroscopy (XPS) was tested using the SSI S-Probe XPS spectrometer. The morphology of the samples was examined by SEM (10 kV, FEI electron microscope). High-resolution TEM (HRTEM) images and energy dispersive X-ray spectrometry (EDS) elemental mapping were carried out at an electron acceleration voltage of 200 kV (FEI Talos F200s).

4. Electrochemical measurements

All electrochemical data were collected on CHI760 electrochemical station (Chenhua, Shanghai). As–prepared samples were as working electrodes, a graphite rod as the counter electrodes and a standard Hg/HgO electrode as the reference electrode. The polarization curve was measured using LSV technology at a scan rate of 5 mV s^{-1}. All LSV curves in this paper use 95 % iR compensation. A mixture of 1 mg catalyst, 0.5 mg carbon black, 200 μL isopropanol, and 5 μL Nafion was sonicated to form a well–dispersed ink, and the dispersion was then coated on a glass carbon electrode (diameter: 5 mm) for electrochemical testing. The double–layer capacitance (C_{dl}) was obtained by cyclic test voltammetry with scan rates ranging from 20 to 100 mV s^{-1}.

5. Photocatalysis section

The photocatalytic process employed Ru@α-MnO_2 NWs (loaded on carbon paper with a surface area of 1×1 cm^2) as both cathode and anode catalysts. The system was powered by a polycrystalline silicon photovoltaic solar cell (with an active area of 0.36 cm^2, a maximum voltage of 2 V, a rated voltage of 2 V, and a short-circuit current of 101 mA) and tested in a two-electrode electrochemical cell.

Results and Discussion

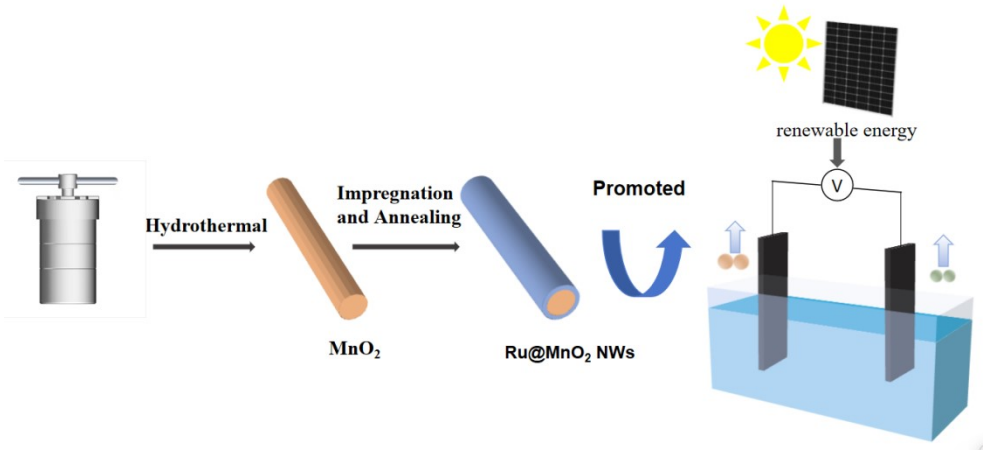

Fig. S1 Schematic illustration of the synthesis process of Ru@MnO_2 and electrode reactions.

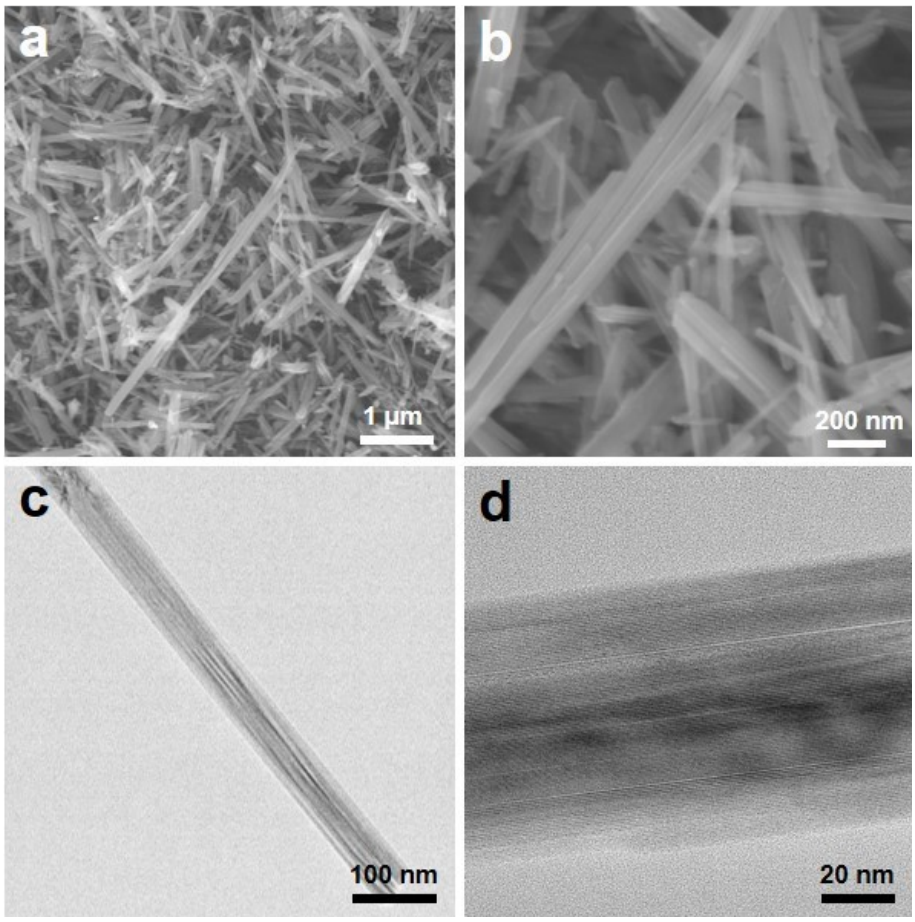

Fig. S2 (a, b) SEM images and (c, d) TEM images of α–MnO_2 NWs.

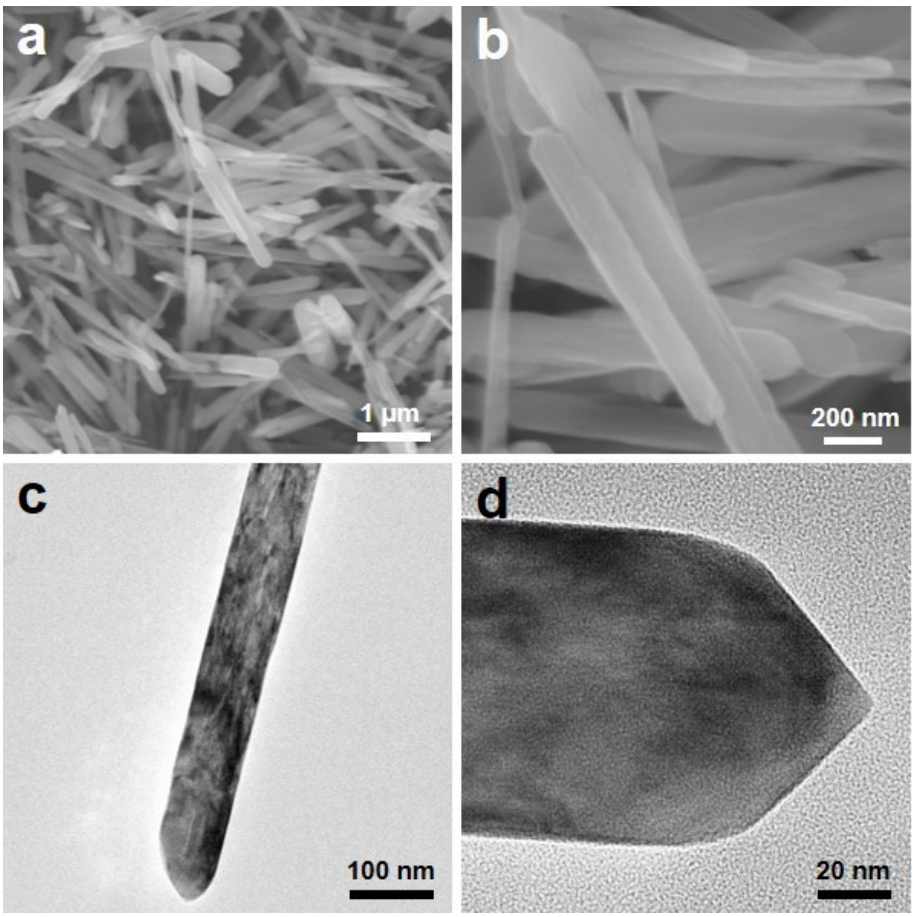

Fig. S3 (a, b) SEM images and (c, d) TEM images of β–MnO_2 NWs.

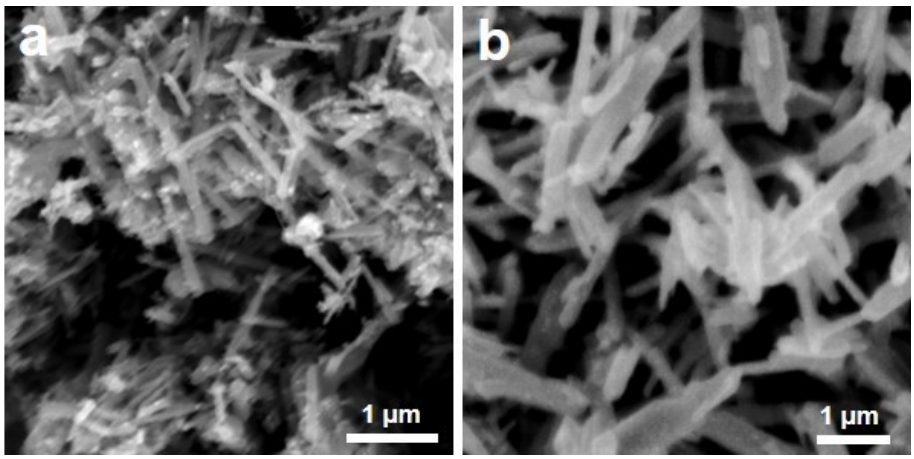

Fig. S4 SEM images of (a) Ru@α-MnO_2 NWs and (b) Ru@β–MnO_2 NWs.

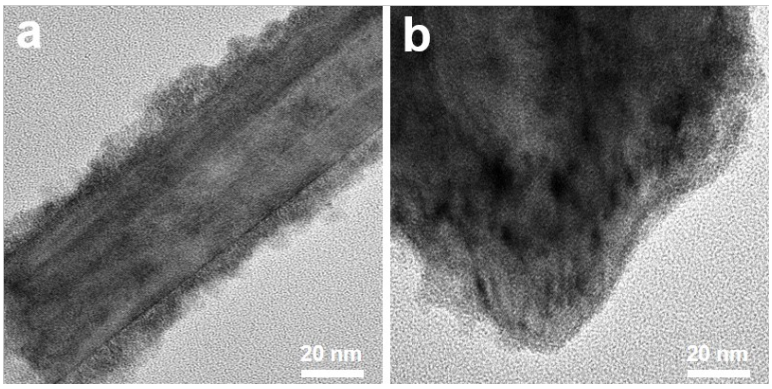

Fig. S5 TEM images of (a) Ru@α–MnO_2 NWs and (b) Ru@β–MnO_2 NWs.

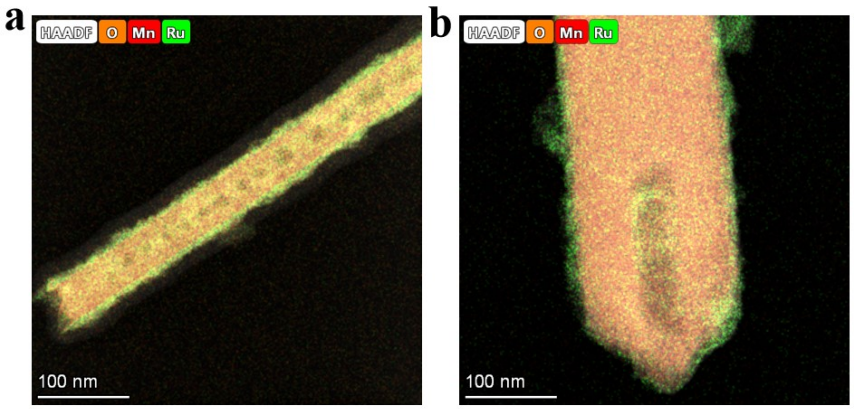

Fig. S6 HADDF images of (a) Ru@α–MnO_2 NWs and (b) Ru@β–MnO_2 NWs.

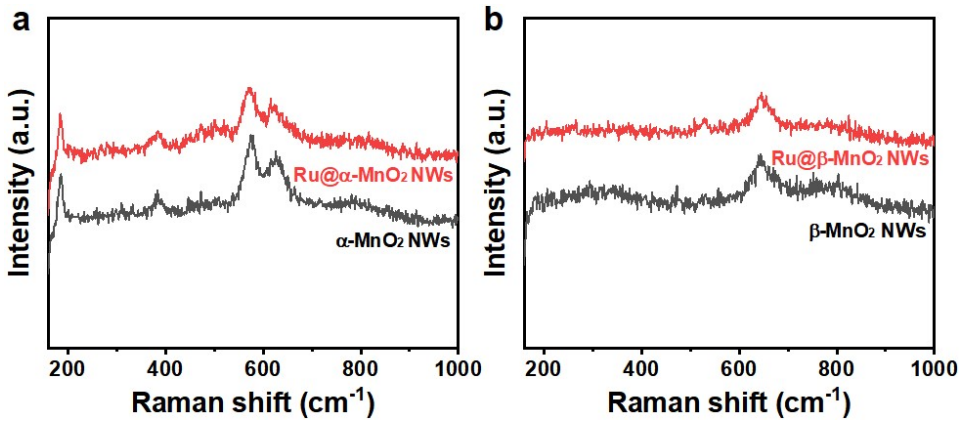

Fig. S7 Raman spectra of (a) α–MnO_2 NWs and Ru@α–MnO_2 NWs and (b) β–MnO_2 NWs and Ru@β–MnO_2 NWs.

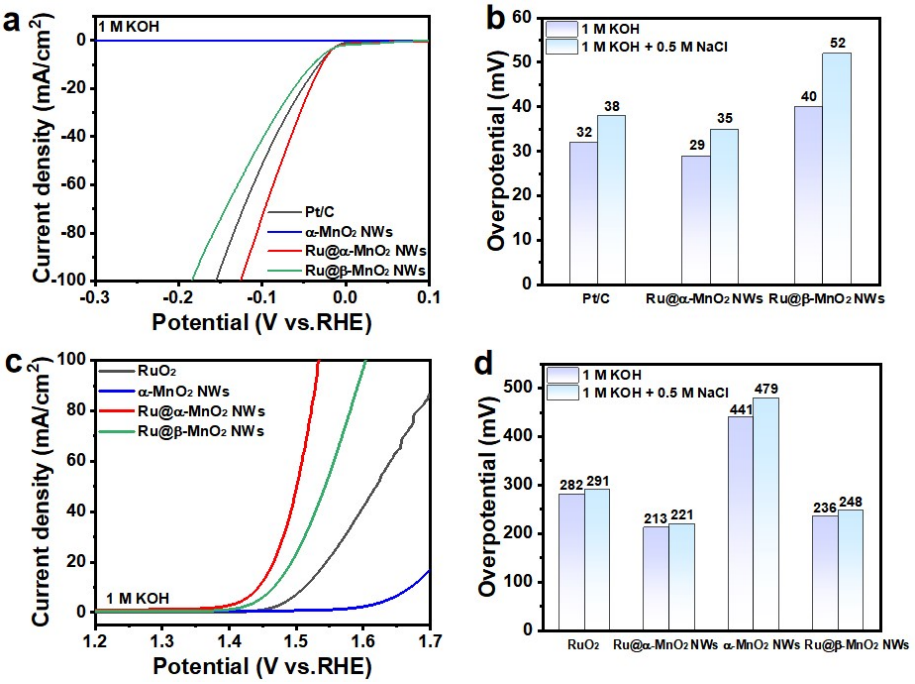

Fig. S8 (a) HER polarization curves and (b) corresponding overpotential (10 mA cm^{-2}) in different electrocatalysts. (c) OER polarization curves and (d) corresponding overpotential (10 mA cm^{-2}) in different electrocatalysts.

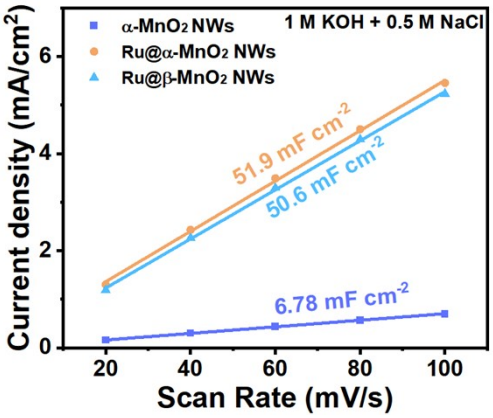

Fig. S9 C_{dl} plots of α–MnO_2 NWs, Ru@α–MnO_2 NWs, and Ru@β–MnO_2 NWs.

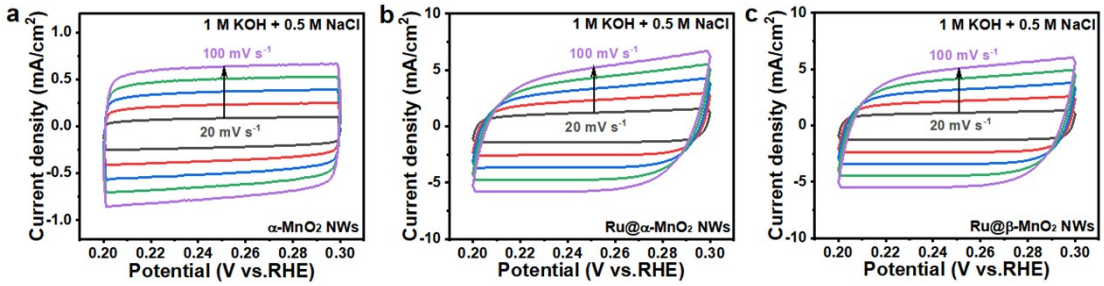

Fig. S10 CV curves of (a) α–MnO_2 NWs, (b) Ru@α–MnO_2 NWs, and (c) Ru@β–MnO_2 NWs in 1 M KOH + 0.5 M NaCl.

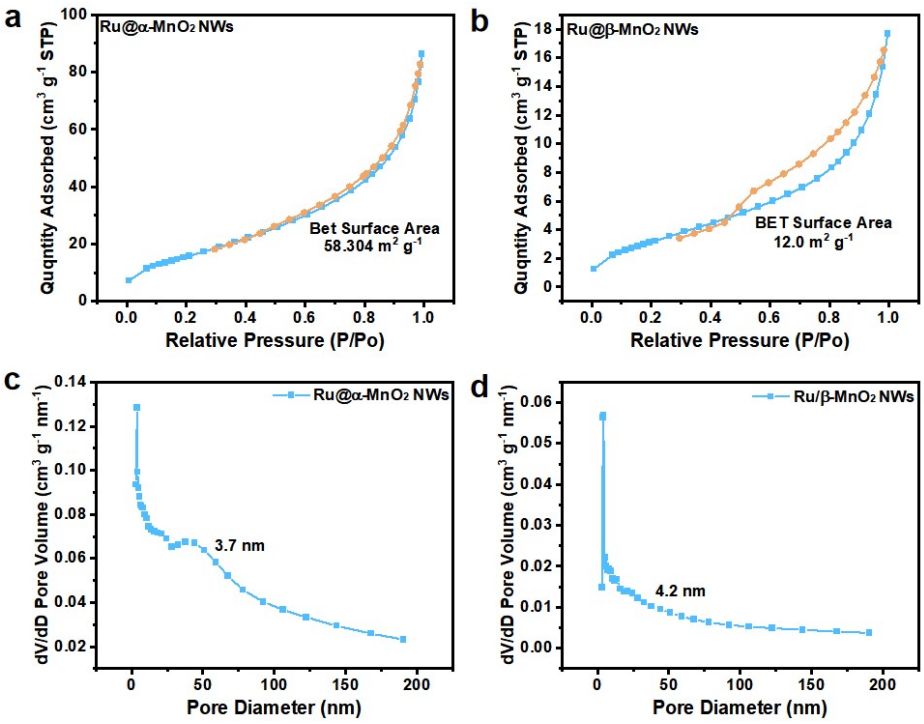

Fig. S11 (a, b) N_2 adsorption–desorption isotherm and (c, d) pore size distribution of (a, b) Ru@α–MnO_2 NWs and (c, d) Ru@β–MnO_2 NWs.

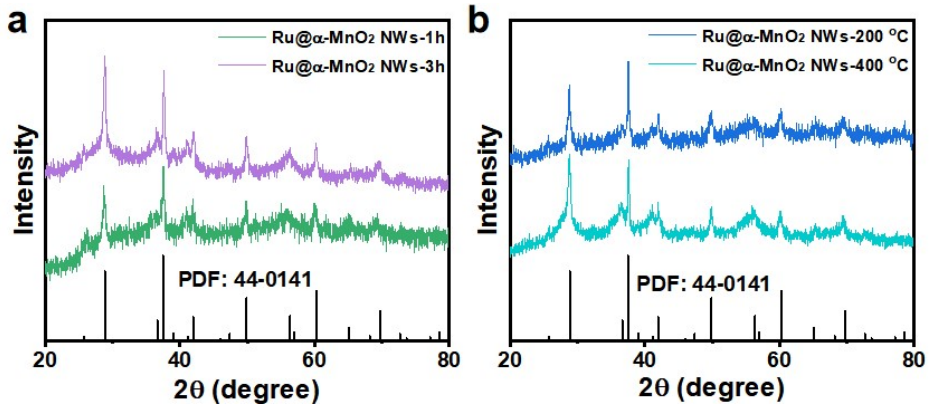

Fig. S12 XRD patterns of (a) Ru@α–MnO_2 NWs–1h and Ru@α–MnO_2 NWs–3h and (b) Ru@α–MnO_2 NWs–200 °C and Ru@α–MnO_2 NWs–400 °C.

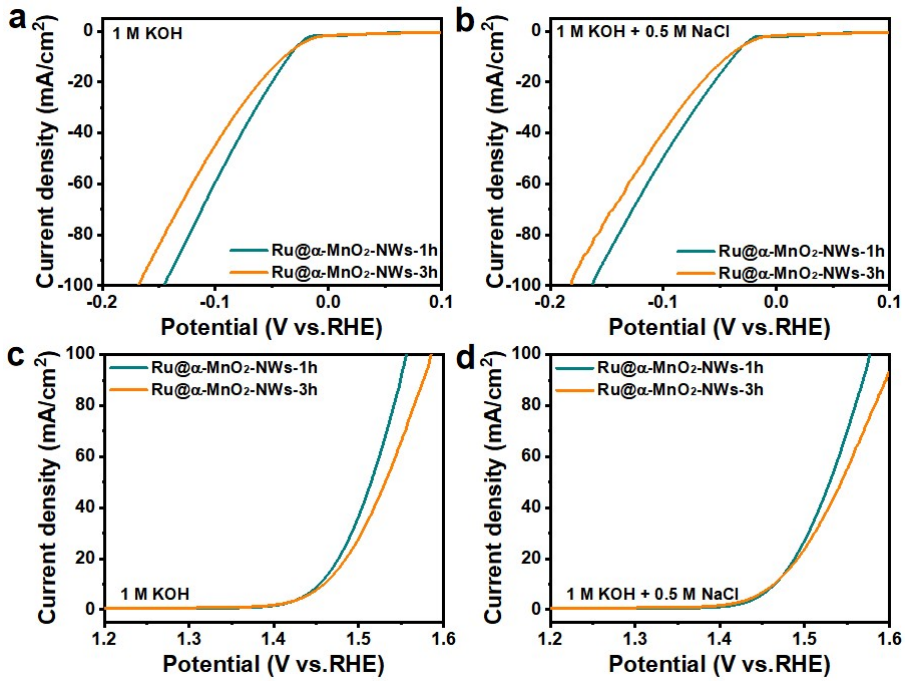

Fig. S13 (a, b) HER and (c, d) OER polarization curves of Ru@α–MnO_2 NWs–1h and Ru@α–MnO_2 NWs–3h in (a, c) 1 M KOH and (b, d) 1 M KOH + 0.5 M NaCl.

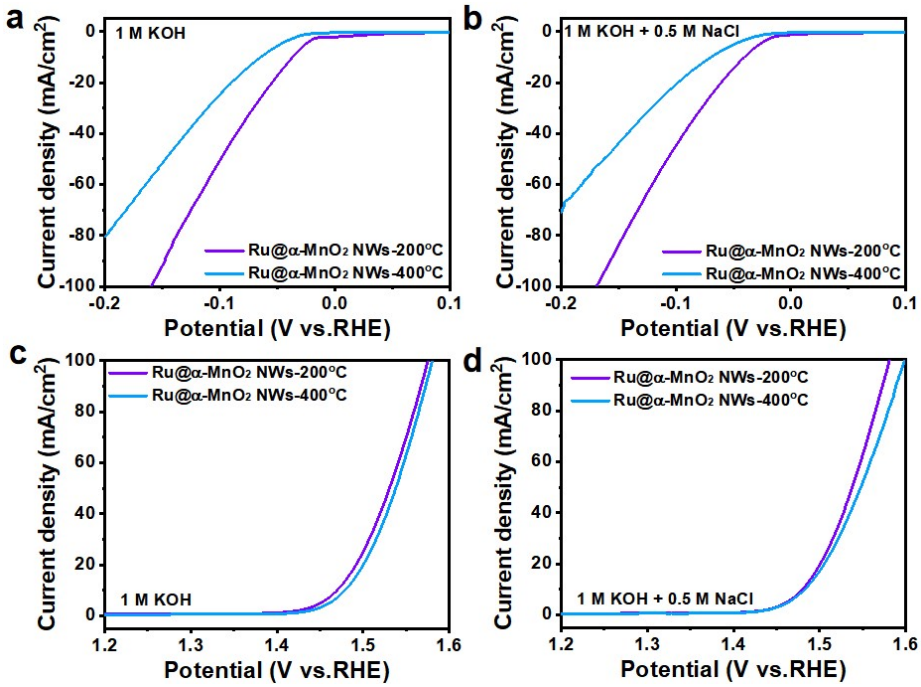

Fig. S14 (a, b) HER and (c, d) OER polarization curves of Ru@α–MnO_2 NWs–200 °C and Ru@α–MnO_2 NWs–400 °C in (a, c) 1 M KOH and (b, d) 1 M KOH + 0.5 M NaCl.

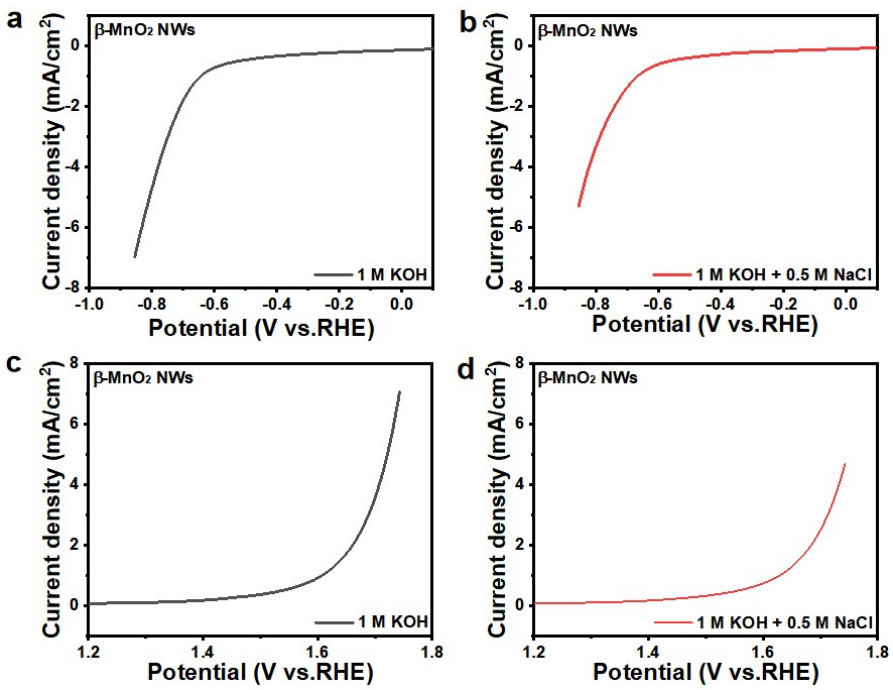

Fig. S15 (a, b) HER and (c, d) OER polarization curves of β–MnO_2 NWs in (a, c) 1 M KOH and (b, d) 1 M KOH + 0.5 M NaCl.

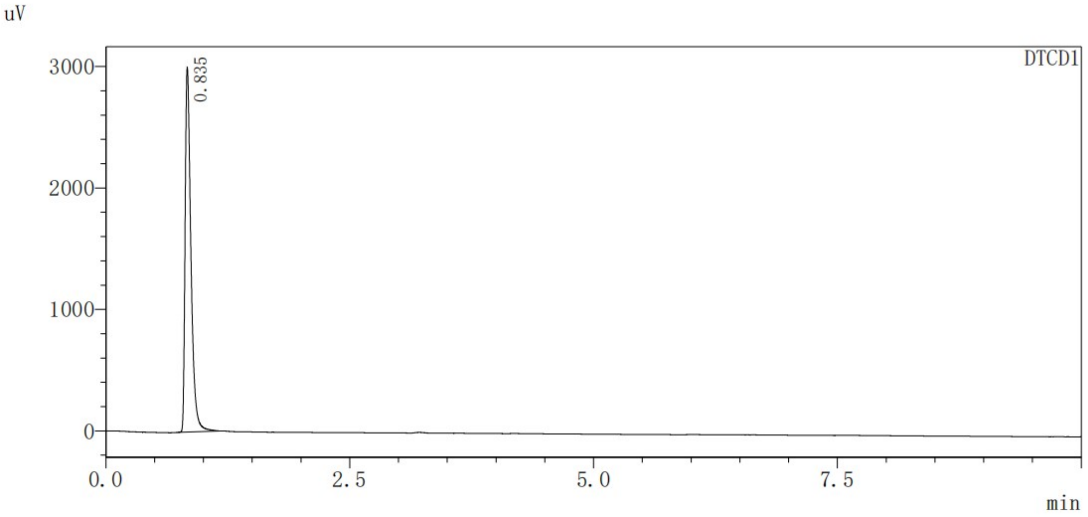

Fig. S16 The Faraday Efficiency (FE) of H_2 for Ru@α-MnO_2 NWs Catalyst.

The calculation method for the Faraday efficiency of the product is as follows:

$FE_{product} = n_{product}\alpha F / Q \times 100\%$ $Q=It$

Where n is the molar amount of the product, α is the number of electrons transferred from one molecule of H_2O to the product, F is 96485 C mol^{-1} (Coulombs per mole), and Q is the total charge passed.

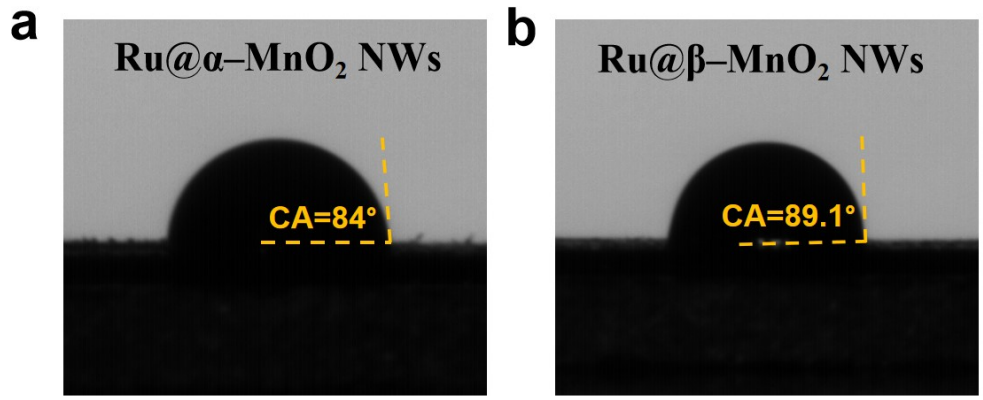

Fig. S17 Contact angle of Ru@α-MnO_2 NWs and Ru@β-MnO_2 NWs.

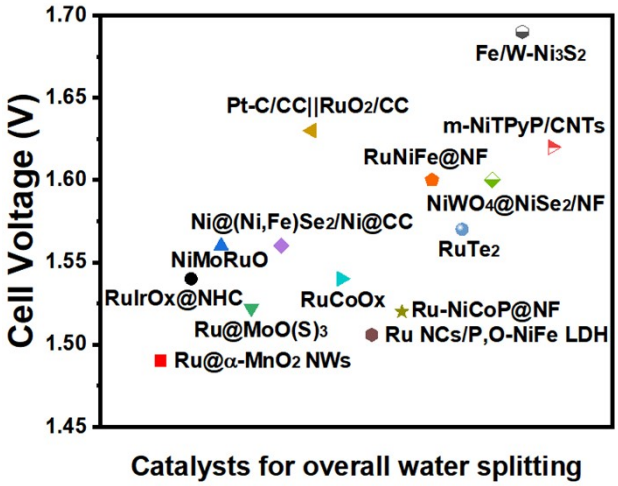

Fig. S18 Comparison with other bifunctional catalysts.

Table S1. Ru@α–MnO_2 NWs, compared with the overall hydrolysis performance of a reported catalyst

Catalyst	Current density	HER (mV)	OER (mV)	Cell Voltage (V)	Reference
Ru@α-MnO_2 NWs	10 mA cm^{-2}	35	221	1.49	This work
RuIrOx@NHC	10 mA cm^{-2}	53	273	1.54	Small. 2024, 20, 2308841.
NiMoRuO	10 mA cm^{-2}	37	280	1.56	Nano Lett. 2023, 23, 1052-1060.
Ru@$MoO(S)_3$	10 mA cm^{-2}	30	265	1.522	Nano Energy. 2022, 100, 107445.
Ni@(Ni,Fe)Se_2/Ni@CC	10 mA cm^{-2}	98	224	1.56	ChemPhysMater. 2024, 3, 320-328.
Pt-C/CC||RuO_2/CC	10 mA cm^{-2}	40	270	1.63	Appl. Catal. B. 2022, 317, 121729.
RuCoOx	10 mA cm^{-2}	37	275	1.54	Nano Lett. 2021, 21, 9633-9641.
Ru NCs/P,O-NiFe LDH	10 mA cm^{-2}	29	175	1.506	Adv. Funct. Mater. 2024, 34, 2310690.
Ru-NiCoP@NF	10 mA cm^{-2}	44	216	1.52	Appl. Catal. B. 2020, 279, 119396.
RuNiFe@NF	10 mA cm^{-2}	62	210	1.60	Chem. Eur. J. 2020, 26, 17091-17096.
$RuTe_2$	10 mA cm^{-2}	34	275	1.57	Appl. Catal. B. 2020, 278, 119281.
$NiWO_4$@$NiSe_2$/NF	10 mA cm^{-2}	132	258	1.60	J. Alloys Compd. 2023, 951, 169941.
Fe/W-Ni_3S_2	10 mA cm^{-2}	174	222	1.69	Small, 2024, 20, 2311770.
m-NiTPyP/CNTs	10 mA cm^{-2}	138	267	1.62	Adv. Mater. 2023, 35, 2210727.